HHS Public Access

Author manuscript

*Curr Biol*. Author manuscript; available in PMC 2017 March 07.

Published in final edited form as:

*Curr Biol*. 2016 March 7; 26(5): 698–706. doi:10.1016/j.cub.2016.01.018.

# The timing of midzone stabilization during cytokinesis depends on myosin II activity and an interaction between INCENP and actin

**Jennifer Landino**[1] and **Ryoma Ohi**[1,†]

[1]Department of Cell and Developmental Biology, Vanderbilt University Medical Center, Nashville, TN, 37232

## SUMMARY

The final steps of cell division are tightly coordinated in space and time but whether mechanisms exist to couple the actin and microtubule (MT) cytoskeletons during anaphase and cytokinesis (C phase) is largely unknown. During anaphase, MTs are incorporated into an anti-parallel array termed the spindle midzone (midzone MTs) while F-actin and non-muscle myosin II, together with other factors, organize into the cleavage furrow [1]. Previous studies in somatic cells have shown that midzone MTs become highly stable after furrows have begun ingression [2], indicating that furrow-to-MT communication may occur. Midzone formation is also inhibited in fly spermatocytes that fail to form a cleavage furrow [3] and during monopolar cytokinesis when myosin contractility is blocked by blebbistatin [4]. We show here that midzone MT stabilization is dependent on actomyosin contraction, suggesting that there is active coordination between furrow ingression and microtubule dynamics. Midzone microtubule stabilization also depends on the kinase activity of Aurora B, the catalytic subunit of the Chromosomal Passenger Complex (CPC), uncovering a feedback mechanism that couples furrowing with microtubule dynamics. We further show that the CPC scaffolding protein INCENP binds actin, an interaction that is important for cytokinesis, and for midzone MT stabilization following furrow ingression. Stabilization of midzone MTs with low amounts of taxol rescues cytokinesis in INCENP actin-binding mutant expressing cells. Collectively, our work demonstrates that the actin and microtubule cytoskeletons are coordinated during cytokinesis, and suggests that the CPC is integral for coupling furrow ingression with midzone microtubule stabilization.

## Graphical Abstract

[†]Author for correspondence: Ryoma Ohi, 4150A MRBIII, 465 21st Avenue South, Nashville, TN 37232, ryoma.ohi@vanderbilt.edu.

**AUTHOR CONTRIBUTIONS**

J.L. and R.O. conceived the project and designed the experiments. J.L. conducted the experiments and performed data analysis. J.L. and R.O. wrote the manuscript.

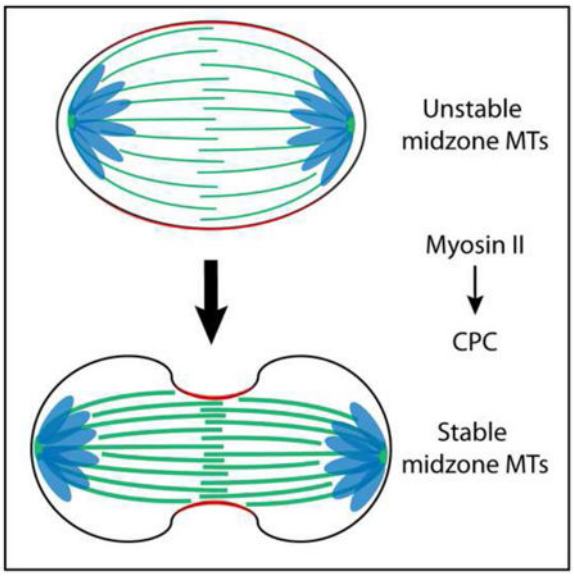


**Keywords**

Cytokinesis; midzone; Aurora B; CPC; actin

## RESULTS

### Midzone MTs are differentially stable during C phase

To investigate the relationship between furrowing and midzone MT stability, we exposed asynchronous HeLa cells to cold temperature (0°C) for 10 minutes prior to fixation. This treatment suggested that midzone MTs become increasingly stable as cells exit mitosis (C phase [5, 6]). Cells that appeared to be in anaphase A at the time of fixation, characterized by chromosome segregation without pole separation and a non-ingressed furrow, were devoid of midzone MTs whereas cells that apparently progressed further, *ie.*, anaphase B and telophase cells, contained cold-stable MTs (Figure 1A). In agreement with previous work [2], cells with cold-stable midzone MTs had invariably initiated furrow ingression; only 5.3 ± 3.2% of non-ingressed cells (mean ± SE, n=70) retained polymer following cold treatment, whereas 82.0 ± 3.5% (n=108) of cells with an ingressed furrow contained polymer (Figure 1B). This qualitative result was unaffected by removal of free tubulin *via* a brief permeabilization step prior to fixation (Figure S1A). Quantitative analysis revealed that the sum intensities of polymeric tubulin fluorescence following cold-treatment in ingressed cells show a positive linear correlation with the degree of furrowing (Figure 1C). This result was unaffected by the presence or absence of free tubulin (Figure S1B). Midzone MTs behaved similarly in the non-transformed RPE-1 cell line (Figures S1C and D).

To better correlate the timing of furrowing with midzone MT stabilization, we next used a live cell assay to monitor midzone MT stability. HeLa cells that simultaneously express GFP-tubulin and mCherry-H2B were challenged during C phase with DMSO or 10 μM nocodazole before or after furrow ingression [2]. DMSO-treated cells progressed through

cytokinesis normally without losing midzone MTs (Figure 1D, Supplemental movie 1A). In contrast, nocodazole caused rapid midzone MT disassembly when added to cells that had not initiated furrowing (Figure 1D, Pre-I, Supplemental movie 1B). The addition of nocodazole to cells that had begun furrowing, however, did not cause widespread midzone MT depolymerization (Figure 1D, Post-I, Supplemental movie 1C). At the terminal time point (7 min following nocodazole addition), pre-ingression cells retained an average of only 16.3 ± 8.6% (mean ± SD, n=10) of the initial midzone MT fluorescence, whereas post-ingression cells retained on average 45.1 ± 16.8% (n=9) of their initial midzone MT fluorescence (Figure 1E). Similar results were obtained using cells expressing mCherry-tubulin (Figures S1E and F). These results indicate that midzone MTs acquire nocodazole resistance after furrowing has initiated, and is consistent with observations made using our fixed cell cold-stability assay.

## Stabilization of midzone MTs requires myosin II activity

Midzone MTs might acquire stability through a time-dependent process or, alternatively, become stabilized by furrowing. To discriminate between these models, we used lamin B immunofluorescence to more precisely judge how long a cell had spent in C phase. Few non-ingressed cells (9.3 ± 1.6%, n=125) had detectable lamin B on chromatin, but this number increased to 95 ± 1.1% (n=123) in ingressed cells (Figure S2A) demonstrating that lamin B is a suitable marker for late-stage C phase cells. We then treated asynchronous cells with 100 μM of the non-muscle myosin II inhibitor blebbistatin to block furrow ingression without perturbing assembly of the contractile array [6]. Although midzones were present in blebbistatin-treated cells at 37°C [6], they were cold-labile (Figure 2A) even in cells containing lamin B-labeled chromatin (Figures 2A and B). Similar results were observed in cells treated with 5 μg/ml cytochalasin B, an actin poison (Figure S2C and E). Again, pre-extraction of free tubulin did not affect these results (Figure S2B and D).

We then tested the relative importance of time spent in C phase *versus* contractility for midzone MT stabilization in live cells using our nocodazole shock assay. As blebbistatin has phototoxic effects when imaged with blue light [7–9], we transiently expressed mCherry-tubulin in HeLa cells to visualize midzone MTs. DIC imaging was also used to determine the degree of chromatin condensation, allowing us to distinguish between cells in early or late stage C phase. Cells were treated with blebbistatin to block furrowing for > 20 min prior to nocodazole addition. Without nocodazole, midzone MTs in early C phase (condensed chromatin as observed by DIC) or late C phase (decondensed chromatin) persisted throughout blebbistatin treatment (Figures 2C and D, Supplemental movies 2A and C). Addition of nocodazole, however, induced midzone MT disassembly during both early and late C phase (Figures 2C and D, Supplemental movies 2B and D). At the terminal time point (6 minutes, 30 seconds), cells early in C phase treated with nocodazole had 26.0 ± 7.2% (n=14) of the initial fluorescence from tubulin polymer. Nocodazole similarly affected cells late in C phase (34.6 ± 9.9%, n=13) indicating that a prolonged C phase does not considerably increase midzone MT stability in the absence of myosin II contractility (Figure 2E). Collectively, these observations suggest that midzone MTs do not become stable as a function of time spent in C phase, but rather that their stability is dependent on myosin II contractility.

### Stabilization of midzone MTs requires Aurora B kinase activity

Aurora B kinase (ABK) is the catalytic component of the Chromosomal Passenger Complex (CPC), a protein complex which also consists of INCENP, Borealin, and Survivin, and plays key roles in multiple aspects of cytokinesis [10]. While the CPC has well-documented functions in cleavage plane specification [11] and promoting midzone assembly [12], its role at the furrow remains unclear. Interestingly, studies of monopolar cytokinesis implicate the CPC in mediating myosin II-dependent cortex-to-MT signaling that promotes the formation of a monopolar midzone [4]. Moreover, the CPC localizes to actin cables in a MT-free zone that connects the cortex to midzone MTs during monopolar cytokinesis [4, 13]. As our data demonstrate a causal relationship between furrow ingression and midzone MT stabilization, and previous work has placed the CPC at the intersection of actin and MT cytoskeletons during cytokinesis, we next investigated ABK as a potential candidate to mediate cortex-to-MT signaling in bipolar midzones.

To test whether ABK might regulate midzone MT stability during C phase, we treated cells for 10 min with the ABK inhibitor 2 μM ZM447439 [14] prior to cold treatment. ZM447439 caused a ~5-fold decrease in the percentage of ingressed cells with cold-stable MTs (15 ± 1.7%, mean ± SE, n=85) compared to control cells (79.3 ± 0.9%, n=123) suggesting that ABK activity is required for midzone MT stabilization after furrow ingression (Figure 3A and B). Pre-extraction of soluble tubulin did not affect the outcome of this experiment (Figure S3A). To demonstrate this in live cells, GFP-tubulin/mCherry-H2B labeled cells were treated with ZM447439 for 5 min prior to imaging or exposure to nocodazole. Under these conditions, ZM447439 treatment alone did not cause midzone MT disassembly in either pre- or post-ingression cells (Figure 3C, Supplemental movies 3A and C). Nocodazole addition, however, caused rapid MT disassembly both before and after furrow ingression (Figure 3C, Supplemental movies 3B and D). Pre-ingression cells treated with ZM447439 maintained only 26.7 ± 10.0% (mean ± SD, n=11) of the initial midzone MT fluorescence after 6 min in nocodazole (Figure 3D). Likewise, post-ingression midzone MTs maintained only 16.9 ± 7.9% (n=10) of the initial fluorescence after nocodazole addition, demonstrating that myosin II-dependent midzone MT stabilization after the initiation of furrowing also requires active ABK.

We also investigated whether myosin II inhibition might alter midzone MT stability by disrupting ABK localization. In fixed cells, we first noted no observable differences in ABK localization in non-ingressed cells compared to ingressed cells suggesting that the change in MT stability observed between these two stages is not due to gross changes in the steady state localization of the kinase (Figure S3B). Additionally, inhibition of myosin II or ABK activity did not prevent ABK from localizing to the division plane (Figure S3C and D) suggesting that changes in midzone MT stability, induced either through contractility or treatment with small molecules, cannot be caused by changes in ABK localization. Brief inhibition of ABK with ZM447439 also did not displace the midzone organizing factors Mklp1 and PRC1 (Figures S3E and F).

## Human INCENP binds actin directly

The localization of ABK to actin cables during monopolar cytokinesis [4] suggests that its function in monopolar midzone formation may require an actin interaction. Interestingly, *Dictyostelium* INCENP has been shown to associate with actin in cells [15], leading us to speculate that human INCENP might also bind actin directly. To examine this possibility, we first analyzed the ability of various GFP-INCENP constructs to co-localize with actin-based structures, marked with mCherry-Utrophin, when exogenously expressed in HeLa cells (Figures S4A and B). A 180 amino acid (aa) fragment of INCENP ($INCENP^{500–680}$) was sufficient to co-localize with actin during mitosis. To confirm the specificity of this co-localization, we treated cells expressing GFP-$INCENP^{500–680}$ with cytochalasin B and found that its localization was disrupted in a manner similar to that of actin (Figure S4B). As INCENP aa residues 500–680 reside in a highly charged region of a single alpha helical domain [16], we hypothesized that INCENP associates with actin through an electrostatic interaction. To test this, and to abrogate a potential INCENP-actin interaction, we generated charge-reversal mutants (lysine/arginine-to-glutamic acid) within amino acid residues 500–680. Charge-reversal of ten residues (K563,R564,R565,R566,K571,K573,R574,R577,R579,K580) abolished co-localization of GFP-$INCENP^{500–680}$ with mCherry-Utrophin in mitotic cells (Figure 4A, $INCENP^{500–680\ CR}$). To determine if INCENP binds actin directly, we purified recombinant $His_6$-$INCENP^{500–680}$ from *E. coli* (Figure S4C) and performed an actin co-sedimentation assay. $His_6$-$INCENP^{500–680}$ sedimented specifically in the presence of F-actin, indicative of a direct interaction. $His_6$-$INCENP^{500–680\ CR}$, however, did not co-sediment with actin, confirming that the mutations that abolish actin co-localization in cells also disrupt direct actin binding *in vitro* (Figure 4B).

## INCENP-actin binding is required for midzone MT stabilization and cleavage furrow ingression

To investigate the role of CPC actin-binding during C phase, we next incorporated the ten charge-reversal mutations into our full-length GFP-INCENP construct (GFP-INCENP CR). We then used a depletion/rescue strategy to substitute endogenous INCENP with either full-length GFP-INCENP or GFP-INCENP CR (Figure S4D). We first analyzed the localization of the CPC in cells expressing wild type GFP-INCENP or GFP-INCENP CR by imaging GFP and ABK. In agreement with previous work [17], GFP-INCENP and ABK both localize to the midzone and the cell cortex in cells expressing wild type GFP-INCENP (Figure 4C), with cortical localization examined in volume projections rotated by 90° In cells expressing GFP-INCENP CR, GFP-INCENP and ABK still localized to the midzone and to the cell cortex, although this mutation appears to partially disrupt CPC distribution along the midzone.

We next assayed midzone MT stability in these cells using exposure to cold temperature (Figure 4D). Similar to unperturbed cells, 86.0 ± 1.5% (mean ± SE, n=84) of ingressed cells expressing wild type GFP-INCENP had cold-stable midzone MTs. However, the percentage of cells with stable midzone MTs decreased ~5-fold in cells expressing GFP-INCENP CR (17.3 ± 3.5%, n=64; Figure 4E). Pre-extraction to remove free tubulin did not change our ability to detect MTs (Figure S4E). This 5-fold decrease in midzone MT stability observed

in ingressed cells expressing GFP-INCENP CR reflects the decrease we observed following ABK inhibition using ZM447439 (Figure 3A), supporting the idea that INCENP-actin interactions are crucial for the CPC to mediate feedback signaling from cortical actin to midzone MTs.

To investigate the role of INCENP-actin binding during cleavage furrow ingression, we used live cell imaging to follow cells depleted of endogenous INCENP and rescued with either GFP-INCENP or GFP-INCENP CR throughout C phase (Supplemental movies 4A and B). We observed that 100 ± 0.0% of cells expressing wild type GFP-INCENP were successful in cleavage furrow ingression (mean ± SE, n=12), validating our approach. In contrast, only 37.8 ± 2.3% of cells expressing GFP-INCENP CR were able to ingress the furrow and form a midbody (n=16; Figure 4F). Myosin II and actin localized normally in cells expressing GFP-INCENP CR (Figure S4F and G), suggesting that furrow ingression failure in GFP-INCENP CR-expressing cells cannot be a consequence of failed actomyosin accumulation.

As cells expressing GFP-INCENP CR have cold-sensitive midzone MTs, we next investigated whether artificially stabilizing MTs would rescue cleavage furrow ingression in these cells. To test this, we incubated cells in the presence of a low dose of taxol (2.5 nM for 30 minutes) prior to imaging, a treatment that did not impede C phase progression in cells expressing wild type GFP-INCENP (Supplemental movie 4C). Cells expressing wild type GFP-INCENP completed cleavage furrow ingression 88.7 ± 11.3% of the time (mean ± SE, n=10) in taxol (Figure 4F). Similarly, cells expressing GFP-INCENP CR also successfully completed cleavage furrow ingression following taxol treatment (91.6 ± 8.3, n=12; Figure 4F, Supplemental movie 4D). To confirm that 2.5 nM taxol altered midzone MT stability during C phase, we used the live cell nocodazole shock assay. HeLa cells stably expressing GFP-tubulin and mCherry-H2B were pre-incubated with DMSO or 2.5 nM taxol for 30 minutes before exposure to 10 μM nocodazole (Figure S4H). In cells pre-incubated with low-dose taxol, midzone MTs were more stable when nocodazole was added before cleavage furrow ingression. At the terminal time point (7 min following nocodazole addition), pre-ingression cells incubated with DMSO retained only 23.9 ± 5.9 % (mean ± SD, n=11) of the initial midzone MT fluorescence, whereas pre-ingression cells incubated with taxol retained on average 38.2 ± 11.9% (n=10) of their initial midzone MT fluorescence (Figure S4I). Taken together these results support the notion that INCENP-actin binding is essential for cytokinesis, and that this interaction is important because it promotes midzone MT stabilization.

## DISCUSSION

Whether actomyosin contractility influences midzone formation during cytokinesis is controversial. Actin disruption eliminates midzone MTs during the meiotic divisions of *Drosophila* spermatocytes [3] and myosin II inhibition prevents midzone formation during monopolar cytokinesis [4]. However, similar perturbations in somatic cells undergoing normal, bipolar cytokinesis [6, 18–20] have yielded conflicting results. Our data show that the midzone MTs of HeLa and RPE-1 cells are stabilized upon furrow initiation in a manner that requires actomyosin contraction, suggesting that furrow ingression impacts bipolar midzone stability rather than assembly. These findings are consistent with previous reports

showing that midzone MTs in somatic cells acquire resistance to nocodazole [2] and pressure [21] during cytokinetic progression. Additionally, our live cell analysis demonstrates that myosin II contractility is only required to initiate the feedback signaling that stabilizes midzone MTs; midzone MTs become nocodazole-resistant once furrowing has begun. While furrowing appears to trigger a unidirectional change in midzone MT stability, the way in which stabilization occurs is not obvious and will be the subject of future work.

Although the mechanism of midzone MT stabilization is not clear, our data identify the CPC as a key mediator of this process; pharmacological inhibition of ABK at any point during cytokinesis results in rapid destabilization of midzone MTs. The importance of CPC actin-binding, *via* INCENP, in promoting midzone MT stabilization after furrow ingression further suggests that the CPC may propagate a midzone MT stabilization signal that originates at the equatorial cortex. Significantly, cortical positioning of the CPC would enable the complex to monitor physical changes in the furrow as it ingresses. Furrow ingression could impact ABK activity at a molecular level, for example through CPC clustering [22] or reductions in dimensionality that affect substrate accessibility [23, 24].

The idea that the CPC participates in a feedback loop that couples the activities of F-actin and MTs during cytokinesis has been suggested previously; Hu *et al.* showed that ABK activity is required for the formation of a midzone during monopolar cytokinesis [4]. Notably, this outcome is different from our observations of bipolar cytokinesis, which we suggest reflects a fundamental difference in the properties of monopolar *versus* bipolar midzones. In accord with this idea, PRC1 and Mklp1 are delocalized in monopolar midzones that do manage to form in the presence of an ABK inhibitor [4], whereas PRC1 and Mklp1 localizations are qualitatively unaffected by ABK inhibition during bipolar cytokinesis (Figures S3E and F). Relative to monopolar midzones, bipolar midzones may be more organizationally robust, perhaps due to the anti-parallel MT crosslinking activity of PRC1 [25, 26] and associated factors, such as KIF4A [27].

An important goal for the future will be to determine the significance of post-furrow ingression midzone MT stabilization during bipolar cytokinesis. Progress will require strategies that selectively alter the functional properties of specific sub-populations of C phase MTs. Here, we developed an INCENP-actin binding mutant as a tool to decrease midzone MT stability after furrowing. Cells expressing this mutant largely fail at cleavage, showing that CPC-actin binding is necessary for cytokinesis. The inability of the INCENP actin-binding mutant to stabilize midzone MTs following furrow initiation appears to be a major underlying defect: Cytokinesis can be rescued with a low-dose of taxol (Figure 4F). Interestingly, the CPC distributes more broadly along the midzone in cells expressing the INCENP CR mutant (Figure 4C), leading us to speculate that INCENP-actin interactions may help to focus the CPC at the division plane. The interaction between Mklp2 and non-muscle myosin II has also been suggested to function in this capacity [28]. While effects on furrowing mediated through astral MTs cannot be ruled out, an intriguing possibility is that positive feedback from midzone MT stabilization promotes furrow closure, creating a double feedback loop that promotes bidirectional CPC-dependent cortex-to-midzone communication.

## Supplementary Material

Refer to Web version on PubMed Central for supplementary material.

## Acknowledgments

We thank Nathan Grega-Larson and Dr. Matt Tyska for the plasmid encoding mCherry-Utrophin, Drs. Susan Wente and Dylan Burnette for antibodies against lamin B and myosin IIA, Megan Dumas for her efforts to image and analyze GFP-INCENP, and members of the P. Ohi lab for critical reading of the manuscript and insightful discussions. This work was supported by National Institutes of Health grant R01GM086610 to R.O. R.O. is a scholar of the Leukemia and Lymphoma Society.

## Abbreviations List

| | |
|---|---|
| **MT** | microtubule |
| **CPC** | Chromosomal Passenger Complex |
| **ABK** | Aurora B kinase |
| **CR** | charge reversal |

## References

1. Green RA, Paluch E, Oegema K. Cytokinesis in animal cells. Annu Rev Cell Dev Biol. 2012; 28:29–58. [PubMed: 22804577]
2. Hu CK, Coughlin M, Field CM, Mitchison TJ. KIF4 regulates midzone length during cytokinesis. Current biology : CB. 2011; 21:815–824. [PubMed: 21565503]
3. Giansanti MG, Bonaccorsi S, Williams B, Williams EV, Santolamazza C, Goldberg ML, Gatti M. Cooperative interactions between the central spindle and the contractile ring during Drosophila cytokinesis. Genes Dev. 1998; 12:396–410. [PubMed: 9450933]
4. Hu CK, Coughlin M, Field CM, Mitchison TJ. Cell polarization during monopolar cytokinesis. The Journal of cell biology. 2008; 181:195–202. [PubMed: 18411311]
5. Canman JC, Hoffman DB, Salmon ED. The role of pre- and post-anaphase microtubules in the cytokinesis phase of the cell cycle. Current biology : CB. 2000; 10:611–614. [PubMed: 10837228]
6. Straight AF, Cheung A, Limouze J, Chen I, Westwood NJ, Sellers JR, Mitchison TJ. Dissecting temporal and spatial control of cytokinesis with a myosin II Inhibitor. Science. 2003; 299:1743–1747. [PubMed: 12637748]
7. Kepiro M, Varkuti BH, Vegner L, Voros G, Hegyi G, Varga M, Malnasi-Csizmadia A. para-Nitroblebbistatin, the non-cytotoxic and photostable myosin II inhibitor. Angewandte Chemie. 2014; 53:8211–8215. [PubMed: 24954740]
8. Mikulich A, Kavaliauskiene S, Juzenas P. Blebbistatin, a myosin inhibitor, is phototoxic to human cancer cells under exposure to blue light. Biochimica et biophysica acta. 2012; 1820:870–877. [PubMed: 22507270]
9. Sakamoto T, Limouze J, Combs CA, Straight AF, Sellers JR. Blebbistatin, a myosin II inhibitor, is photoinactivated by blue light. Biochemistry. 2005; 44:584–588. [PubMed: 15641783]
10. Carmena M, Wheelock M, Funabiki H, Earnshaw WC. The chromosomal passenger complex (CPC): from easy rider to the godfather of mitosis. Nature reviews Molecular cell biology. 2012; 13:789–803. [PubMed: 23175282]
11. Nguyen PA, Groen AC, Loose M, Ishihara K, Wuhr M, Field CM, Mitchison TJ. Spatial organization of cytokinesis signaling reconstituted in a cell-free system. Science. 2014; 346:244–247. [PubMed: 25301629]
12. Kaitna S, Mendoza M, Jantsch-Plunger V, Glotzer M. Incenp and an aurora-like kinase form a complex essential for chromosome segregation and efficient completion of cytokinesis. Current biology : CB. 2000; 10:1172–1181. [PubMed: 11050385]

13. Canman JC, Cameron LA, Maddox PS, Straight A, Tirnauer JS, Mitchison TJ, Fang G, Kapoor TM, Salmon ED. Determining the position of the cell division plane. Nature. 2003; 424:1074–1078. [PubMed: 12904818]
14. Ditchfield C, Johnson VL, Tighe A, Ellston R, Haworth C, Johnson T, Mortlock A, Keen N, Taylor SS. Aurora B couples chromosome alignment with anaphase by targeting BubR1, Mad2, and Cenp-E to kinetochores. The Journal of cell biology. 2003; 161:267–280. [PubMed: 12719470]
15. Chen Q, Lakshmikanth GS, Spudich JA, De Lozanne A. The localization of inner centromeric protein (INCENP) at the cleavage furrow is dependent on Kif12 and involves interactions of the N terminus of INCENP with the actin cytoskeleton. Molecular biology of the cell. 2007; 18:3366–3374. [PubMed: 17567958]
16. Samejima K, Platani M, Wolny M, Ogawa H, Vargiu G, Knight PJ, Peckham M, Earnshaw WC. The INCENP Coil is a Single Alpha Helical (SAH) Domain that Binds Directly to Microtubules and is Important for CPC Localization and Function in Mitosis. The Journal of biological chemistry. 2015
17. Earnshaw WC, Cooke CA. Analysis of the distribution of the INCENPs throughout mitosis reveals the existence of a pathway of structural changes in the chromosomes during metaphase and early events in cleavage furrow formation. Journal of cell science. 1991; 98(Pt 4):443–461. [PubMed: 1860899]
18. Aubin JE, Osborn M, Weber K. Inhibition of cytokinesis and altered contractile ring morphology induced by cytochalasins in synchronized PtK2 cells. Experimental cell research. 1981; 136:63–79. [PubMed: 7197632]
19. Cimini D, Fioravanti D, Tanzarella C, Degrassi F. Simultaneous inhibition of contractile ring and central spindle formation in mammalian cells treated with cytochalasin B. Chromosoma. 1998; 107:479–485. [PubMed: 9914380]
20. Savoian MS, Earnshaw WC, Khodjakov A, Rieder CL. Cleavage furrows formed between centrosomes lacking an intervening spindle and chromosomes contain microtubule bundles, INCENP, and CHO1 but not CENP-E. Molecular biology of the cell. 1999; 10:297–311. [PubMed: 9950678]
21. Salmon ED, Goode D, Maugel TK, Bonar DB. Pressure-induced depolymerization of spindle microtubules. III. Differential stability in HeLa cells. The Journal of cell biology. 1976; 69:443–454. [PubMed: 1262399]
22. Kelly AE, Sampath SC, Maniar TA, Woo EM, Chait BT, Funabiki H. Chromosomal enrichment and activation of the aurora B pathway are coupled to spatially regulate spindle assembly. Developmental cell. 2007; 12:31–43. [PubMed: 17199039]
23. Noujaim M, Bechstedt S, Wieczorek M, Brouhard GJ. Microtubules accelerate the kinase activity of Aurora-B by a reduction in dimensionality. PloS one. 2014; 9:e86786. [PubMed: 24498282]
24. Rosasco-Nitcher SE, Lan W, Khorasanizadeh S, Stukenberg PT. Centromeric Aurora-B activation requires TD-60, microtubules, and substrate priming phosphorylation. Science. 2008; 319:469–472. [PubMed: 18218899]
25. Bieling P, Telley IA, Surrey T. A minimal midzone protein module controls formation and length of antiparallel microtubule overlaps. Cell. 2010; 142:420–432. [PubMed: 20691901]
26. Subramanian R, Wilson-Kubalek EM, Arthur CP, Bick MJ, Campbell EA, Darst SA, Milligan RA, Kapoor TM. Insights into antiparallel microtubule crosslinking by PRC1, a conserved nonmotor microtubule binding protein. Cell. 2010; 142:433–443. [PubMed: 20691902]
27. Kurasawa Y, Earnshaw WC, Mochizuki Y, Dohmae N, Todokoro K. Essential roles of KIF4 and its binding partner PRC1 in organized central spindle midzone formation. The EMBO journal. 2004; 23:3237–3248. [PubMed: 15297875]
28. Kitagawa M, Fung SY, Onishi N, Saya H, Lee SH. Targeting Aurora B to the equatorial cortex by MKlp2 is required for cytokinesis. PloS one. 2013; 8:e64826. [PubMed: 23750214]

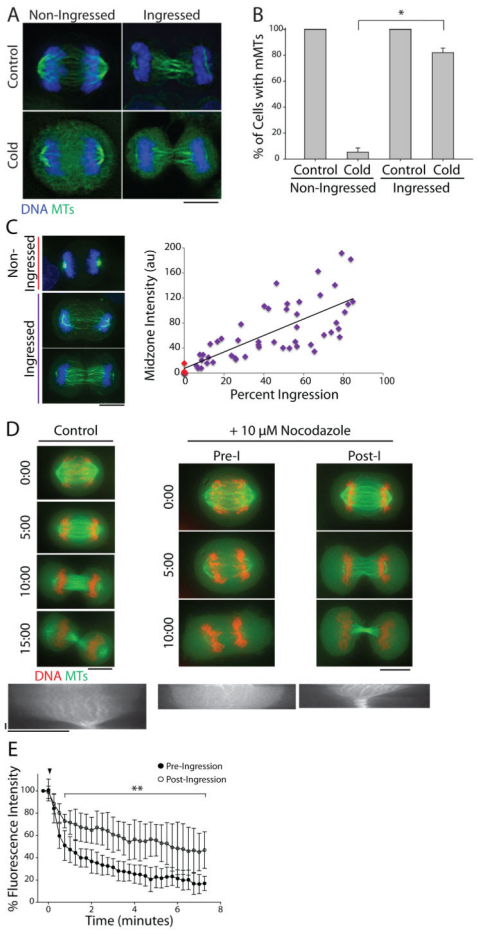


**Figure 1. Midzone MTs are differentially stable during C phase**

A) Maximum z-projections of untreated (top) or cold-treated (bottom) HeLa cells in C phase with non-ingressed or ingressed cleavage furrows. Cells were stained with antibodies against tubulin (green) and counterstained with Hoechst 33342 to visualize DNA (blue). Scale bar, 10 µm. B) Quantification of the percentage of cells with midzone MTs (mMTs) before and after cold treatment as described in A). Data represent mean ± SE. n > 150 cells from three independent experiments, * = $p < 0.005$. C) Left: Maximum z-projections of cold-treated HeLa cells permeabilized prior to fixation to extract free tubulin. Cells were otherwise fixed and stained as described in A). Dashed lines indicate cell boundary. Scale bar, 10 µm. Right: Quantification of midzone MT fluorescence intensity after cold treatment in non-ingressed (red) and ingressed (purple) cells plotted as a function of the percent furrow ingression. Cells were fixed after pre-extraction of free tubulin. (n=54). D) Top: Single z-plane micrographs taken from time lapse movies of HeLa cells expressing GFP-tubulin (green) and mCherry-H2B (red) exiting mitosis in the presence of DMSO (control) or 10 µM nocodazole. Time is indicated in min relative to the initial frame. Dashed lines were used to generate kymographs. Scale bars, 10 µm. Bottom: Kymographs of GFP-tubulin fluorescence across the division plane during C phase. Arrowheads (white) indicate time point of nocodazole addition. Scale bars, 2.5 min (x axis) and 10 µm (y axis). E) Quantification of midzone MT fluorescence intensity in pre- and post-ingression cells treated with 10 µM

nocodazole. Arrowhead (black) indicates the time of nocodazole addition. Data represent mean ± SD. n=10 (pre-ingression) and 9 (post-ingression) from three independent experiments, ** = $p < 0.01$. See also Figure S1.

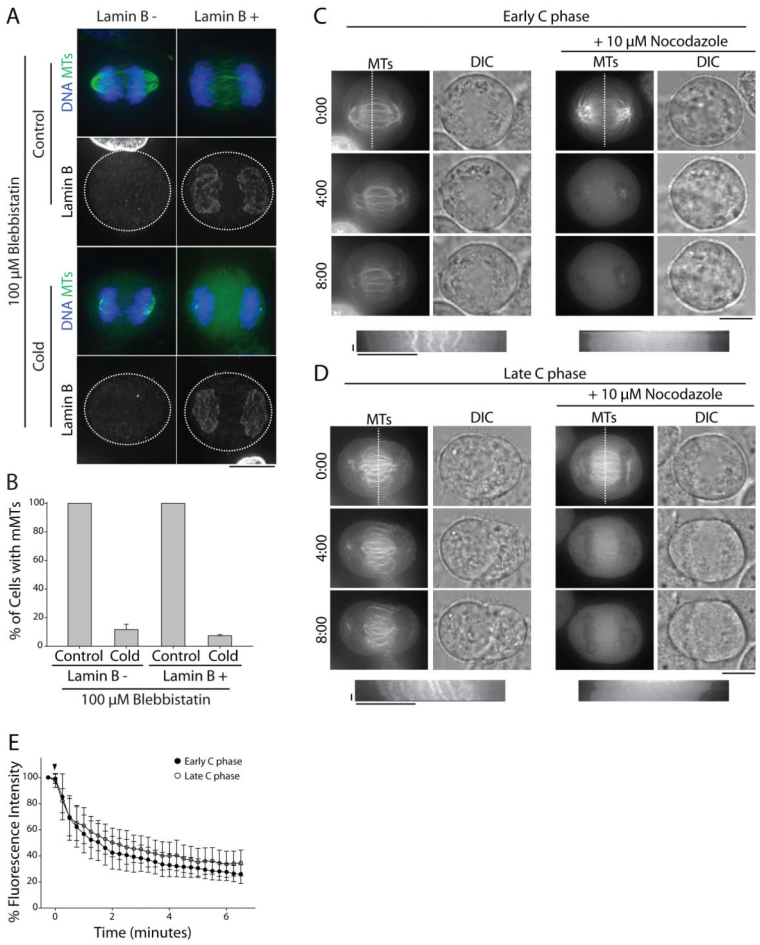


**Figure 2. Midzone MT stabilization requires non-muscle myosin II activity**

A) Maximum z-projections of cells treated with 100 μM blebbistatin prior to fixation (top) or cold treatment (bottom). Cells were stained with antibodies to lamin B (single channels) to mark the nuclear envelope and tubulin (green). DNA was counterstained with Hoechst 33342 (blue). Scale bar, 10 μm. B) Quantification of the percentage of blebbistatin-treated cells with midzone MTs before and after cold treatment as described in A). Data represent mean ± SE, n > 200 cells from three independent experiments. C) Top: Single z-plane micrographs of HeLa cells expressing mCherry-tubulin in early C phase, as judged by the degree of chromatin condensation. Cells were treated with 100 μM blebbistatin prior to addition of 10 μM nocodazole. Time is indicated in min relative to the initial frame. Dashed lines were used to generate kymographs. Scale bar, 10 μm. Bottom: Kymographs of mCherry-tubulin fluorescence across the division plane during C phase. Arrowheads (white) indicate time of nocodazole addition. Scale bars, 2.5 min (x axis) and 10 μm (y axis). D) Top: Single z-plane micrographs of HeLa cells expressing mCherry-tubulin in late C phase, as judged by the lack of condensed chromatin. Cells were treated with 100 μM blebbistatin prior to addition of 10 μM nocodazole. Time is indicated in min relative to the initial frame. Dashed lines were used to generate kymographs. Scale bar, 10 μm. Bottom: Kymographs of mCherry-tubulin fluorescence across the division plane during C phase. Arrowheads (white) indicate time of nocodazole addition. Scale bars, 2.5 min (x axis) and 10 μm (y axis). E)

Quantification of midzone MT fluorescence intensity in early and late C phase cells treated with 100 μM blebbistatin and 10 μM nocodazole. Arrowhead (black) indicates time of nocodazole addition. Data represent mean ± SD. n=14 (early anaphase) and 13 (late anaphase), from three independent experiments. See also Figure S2.

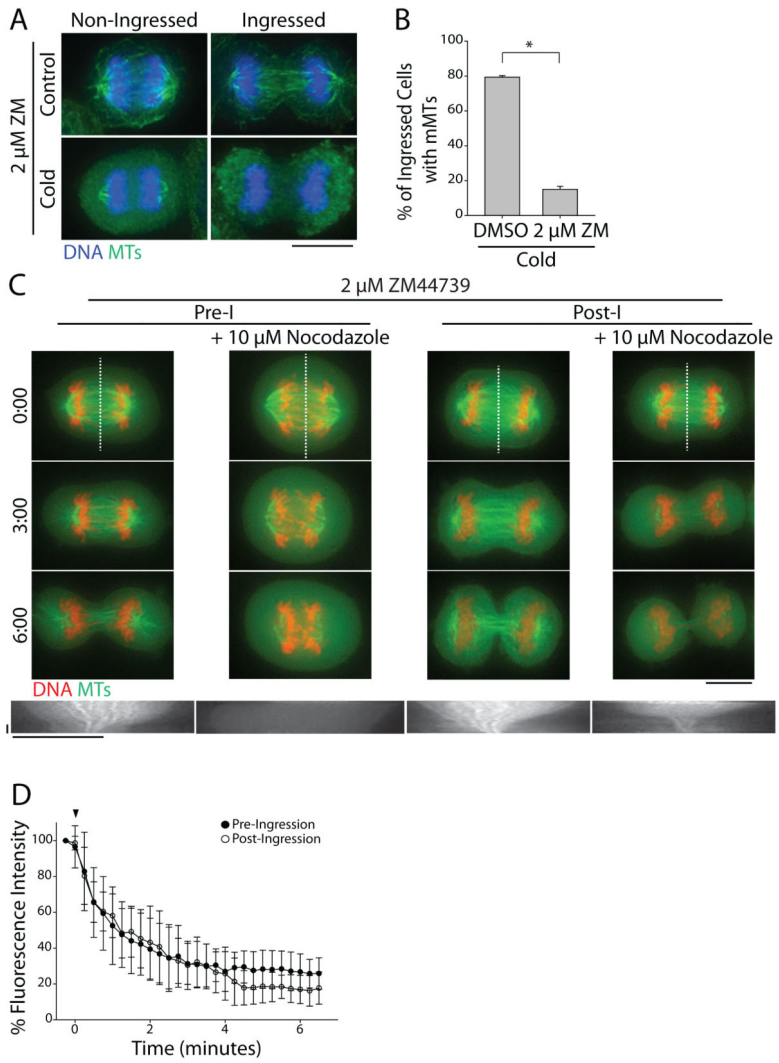


**Figure 3. ABK activity is required for midzone MT stabilization**

A) Maximum z-projections of cells treated with 2 μM ZM447439 (ZM) prior to fixation (top) or cold treatment (bottom). Cells were stained with antibodies to tubulin (green) and DNA was counterstained with Hoechst 33342 (blue). Scale bar, 10 μm. B) Quantification of the percentage of ingressed cells with midzone MTs after treatment with DMSO or 2 μM ZM447439 and cold. Data represent mean ± SE, n > 200 cells from three independent experiments, * = $p < 0.005$. C) Top: Single z-plane micrographs taken from time lapse movies of pre- and post-ingression HeLa cells expressing GFP-tubulin (green) and mCherry-H2B (red) treated with 2 μM ZM447439 with or without 10 μM nocodazole. Time is indicated in min relative to the initial frame. Dashed lines were used to generate kymographs. Scale bar, 10 μm. Bottom: Kymographs of GFP-tubulin fluorescence across the division plane during C phase. Arrowheads (white) indicate time of nocodazole addition. Scale bars, 2.5 minutes (x axis) and 10 μm (y axis). D) Quantification of midzone MT fluorescence intensity in pre- and post-ingression cells treated with 2 μM ZM447439 and 10 μM nocodazole. Arrowhead (black) indicates time of nocodazole addition. Data represent

mean ± SD. n=11 (pre-ingression), and 10 (post-ingression) from three independent experiments. See also Figure S3.

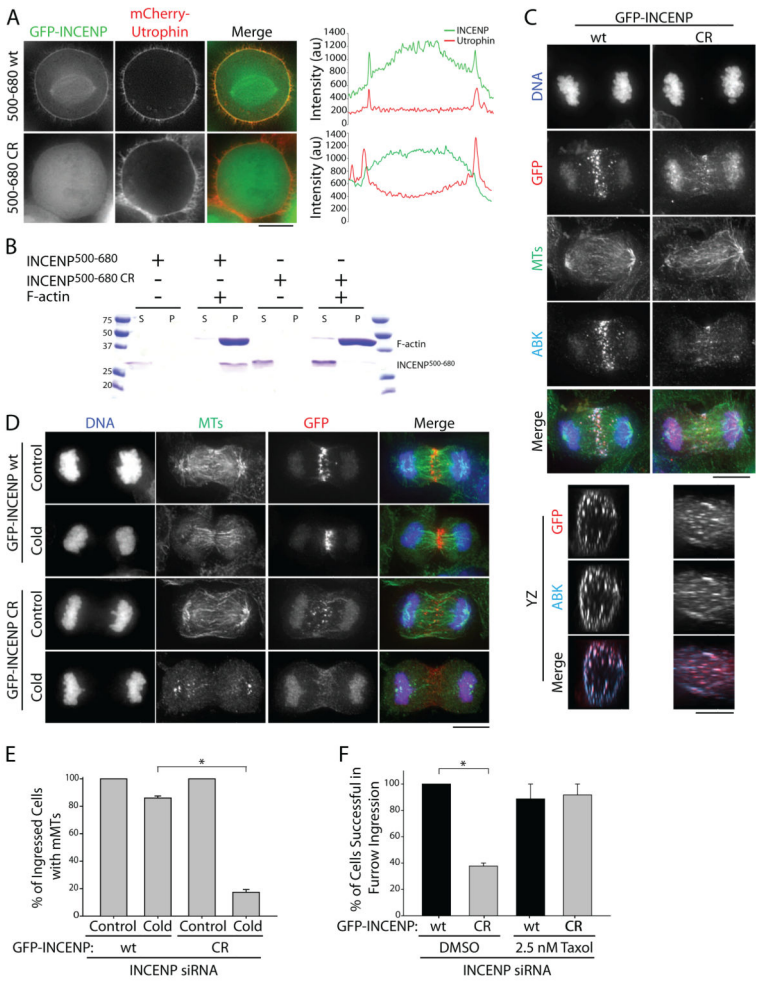


**Figure 4. INCENP actin-binding promotes midzone MT stabilization and furrow ingression**

A) Single z-plane micrographs of HeLa cells transiently expressing mCherry-Utrophin to mark actin (red) and GFP-INCENP$^{500–680}$ fragments (green) containing the wild type (wt) INCENP sequence or charge reversal (CR) mutations. Dashed lines were used to generate line scans. Scale bar, 10 μm. B) Coomassie-stained gel showing an actin co-sedimentation assay using recombinant wt or CR His$_6$-INCENP$^{500–680}$. Supernatant (S) and pellet (P) fractions are indicated. Molecular weight standards are indicated in kDa. C) Maximum z-projections of the X and Y dimensions (top panels) and volume projections of Y and Z dimensions (bottom panels) of GFP-INCENP (wt or CR, red) in HeLa cells depleted of endogenous INCENP using a siRNA targeting the 3′ UTR of INCENP. Cells were stained with antibodies against tubulin (green), and ABK (teal). DNA (blue) was counterstained with Hoechst 33342. Scale bar, 10 μm. D) Maximum z-projections of HeLa cells depleted of endogenous INCENP and rescued with full-length GFP-INCENP (top) or GFP-INCENP CR (bottom) prior to fixation or cold-treatment. Cells were stained with antibodies against tubulin (green) and GFP (red). DNA was counterstained with Hoechst 33342 (blue). Scale bar, 10 μm. E) Quantification of the percent of cells with midzone MTs before and after cold-treatment as described in D). Data represent mean ± SE. n = 148 cells from three independent experiments, * = $P < 0.005$. F) Quantification of the percentage of cells

expressing GFP-INCENP wt or CR that successfully completed furrow ingression. HeLa cells were depleted of endogenous INCENP and rescued with GFP-INCENP wt or the charge reversal mutant (CR). Cells were pre-incubated with DMSO or 2.5 nM Taxol for 30 mins prior to imaging. Data represent mean ± SE. n= 12 (wt, DMSO), 16 (CR, DMSO), 10 (wt, Taxol), and 12 (CR, Taxol) cells from three independent experiments, * = $p < 0.05$. See also Figure S4.